The evolution and development of cranial form in *Homo sapiens*

Daniel E. Lieberman*†, Brandeis M. McBratney*, and Gail Krovitz‡

*Department of Anthropology, Harvard University, 11 Divinity Avenue, Cambridge, MA 02138; and ‡Department of Anthropology, George Washington University, 2110 G Street NW, Washington, DC 20052

Edited by Henry C. Harpending, University of Utah, Salt Lake City, UT, and approved November 26, 2001 (received for review August 20, 2001)

Despite much data, there is no unanimity over how to define *Homo sapiens* in the fossil record. Here, we examine cranial variation among Pleistocene and recent human fossils by using a model of cranial growth to identify unique derived features (autapomorphies) that reliably distinguish fossils attributed to "anatomically modern" *H. sapiens* (AMHS) from those attributed to various taxa of "archaic" *Homo* spp. (AH) and to test hypotheses about the changes in cranial development that underlie the origin of modern human cranial form. In terms of pattern, AMHS crania are uniquely characterized by two general structural autapomorphies: facial retraction and neurocranial globularity. Morphometric analysis of the ontogeny of these autapomorphies indicates that the developmental changes that led to modern human cranial form derive from a combination of shifts in cranial base angle, cranial fossae length and width, and facial length. These morphological changes, some of which may have occurred because of relative size increases in the temporal and possibly the frontal lobes, occur early in ontogeny, and their effects on facial retraction and neurocranial globularity discriminate AMHS from AH crania. The existence of these autapomorphies supports the hypothesis that AMHS is a distinct species from taxa of "archaic" *Homo* (e.g., *Homo neanderthalensis*).

Paradoxically, our own species, *Homo sapiens,* is one of the most poorly defined species of hominids. The recent human fossil record has a confusing pattern of variation, with numerous vaguely defined taxa (e.g., "archaic" *H. sapiens*, "modern" *H. sapiens*, *Homo heidelbergensis*, *Homo helmei*, *Homo rhodesiensis*), most of which are not widely accepted. A major source of this confusion is the lack of established unique derived features (autapomorphies) of "anatomically modern" *H. sapiens* (AMHS). The most frequently used diagnosis for AMHS is Day and Stringer's (1), which is based solely on cranial features (listed in Table 1), and which has since been expanded and scrutinized (2–6). However, there are at least two major problems with the diagnostic features in Table 1. First, most of the features are difficult to use as phylogenetic characters because they describe cranial vault globularity, and are thus not structurally or developmentally independent. A second, more fundamental problem is their failure to discriminate reliably between "archaic" *Homo* spp. (AH) and AMHS. Many recent human crania fall outside the supposed range of AMHS variation for some features, and a few skulls generally attributed to AH fall within the range of AMHS variation (7, 8). Many researchers (e.g., ref. 9) thus consider *H. sapiens* to be a morphologically diverse species with archaic and anatomically modern grades.

Although *H. sapiens* may include anatomically modern and archaic variants, an increasingly popular view is that AMHS is a distinct species. The best support for this hypothesis comes from genetic evidence for an African origin of extant human populations between 100,000 and 200,000 years ago, and for divergence between humans and Neanderthals about 500,000–600,000 years ago (10–12). Testing this hypothesis by using cranial features, however, is a challenge because of the substantial integration that occurs among the various semi-independent units of the cranium (13, 14). Recent evolutionary developmental studies show that major changes in form associated with speciation typically result from ontogenetically early alterations in the regulation of growth, leading to multiple correlated phenotypic novelties (15, 16). Thus, interactions at multiple hierarchical levels of development—from individual genes to structural modules (integrated suites of characters that grow as a unit)—confound efforts to define basic independent characters. Yet such autapomorphies are predicted to exist if AMHS evolved as a separate lineage from AH.

We test here the hypothesis that AMHS is a distinct species in a phylogenetic sense, recognizable on the basis of one or more autapomorphies, against the null hypothesis that AMHS has no autapomorphies, indicating inclusion in a separate lineage. To this end, we report three analyses that examine cranial variation in recent *Homo* by using a developmental model of cranial evolution. First, we use factor analysis to identify structurally important combinations of variables that covary among AMHS crania. Second, we use ANOVA and comparisons of sample ranges to test whether these structural differences discriminate reliably between AMHS and AH. Finally, we combine two morphometric analyses to investigate hypotheses about the developmental shifts that influence the major structural differences between AH and AMHS cranial form. First, by comparing the pattern of three-dimensional cranial shape in adult AH and AMHS by using landmarks that include major loci of cranial growth, we identify cranial regions that appear to contribute to shape differences between the taxa. Second, we test whether variables that quantify the same shape differences between AH and AMHS contribute during ontogeny to the major cranial differences between humans and our closest extant relatives, chimpanzees.

Materials and Methods

Materials. The majority of the previously proposed diagnostic cranial characters of AMHS listed in Table 1 and several other variables (see below) were measured by using external landmarks from several samples: 100 recent *H. sapiens* (50 of each sex) from five craniofacially diverse populations (from Australia, China, Egypt, Italy, and West Africa; for details, see ref. 17); 10 relatively complete Late Pleistocene fossils commonly classified as early AMHS (Cro Magnon 1, Jebel Irhoud 1, Liujiang, Minatogawa 1, Obercassel 1, Predmosti 4, Qafzeh 6, Qafzeh 9, Skhul V, and Zhoukoudian 101); and nine relatively complete crania typically assigned to AH (but not *H. erectus*) comprising five Neanderthals (Gibraltar 1, Guattari, La Chapelle aux Saints, La Ferrassie 1, and Shanidar 1), and four crania usually attributed to *H. heidelbergensis* or *H. rhodesiensis* (Bodo, Dali, Broken Hill, and Petralona). Fossil crania lacking the upper face were not included. All external measurements were taken from casts at the American Museum of Natural History (New York), with the exception of the recent human sample and Skhul V, which were taken from original specimens. Geometric morphometric comparisons of cranial differences between AH and AMHS were computed from two- and three-dimensional landmarks digitized from computed tomography (CT) scans of four adult fossil crania (Bodo, Broken Hill, Gibraltar

This paper was submitted directly (Track II) to the PNAS office.

Abbreviations: AMHS, anatomically modern *Homo sapiens*; AH, archaic *Homo* spp.; TPS, thin plate spline; EDMA, Euclidean distance matrix analysis.

†To whom reprint requests should be addressed. E-mail: danlieb@fas.harvard.edu.

 www.pnas.org/cgi/doi/10.1073/pnas.022440799

Table 1. Major cranial features traditionally used to diagnose anatomically modern *Homo sapiens*

Diagnostic feature (from refs. 1 and 2)	Diagnostic metric (if present)
Short high vault	Basibregmatic height/glabello-occipital length ≥ 0.70*
Parietals long and curved in mid-saggital plane	Parietal angle (PAA) ≤ 138°*
Parietal arch high and wide in coronal plane	Bregma-asterion chord/biasterionic breadth ≥ 1.19*
Occipital bone long, narrow, not markedly projecting	Occipital angle (OCA) ≥ 114°*
High frontal angle	Frontal angle (FRA) ≤ 134°*
Weak, noncontinuous supraorbital torus divided into medial and lateral portions	Relative size of glabella, supraciliary ridges, and lateral trigones (ST 1–5)†
Canine fossa present	Inferior perimeter of zygomatic process retracted relative to superior (orbital) perimeter*

*From ref. 1.
†From ref. 6, pp. 344–346.

1, and Guattari) and four fairly robust recent adult male *H. sapiens* (two Australian, two Native American) from the National Museum of Natural History (Smithsonian Institution, Washington, DC). Two-dimensional landmarks were digitized from lateral radiographs of a longitudinal study of six male and six female recent *H. sapiens* from the Denver Growth Study (details in ref. 18) and from lateral radiographs of a cross-sectional sample of *Pan troglodytes* (details in ref. 18). All radiographs were compared at three ontogenetic stages: stage I, 50% through the neurocranial growth phase (≈3 years in *H. sapiens* and 1.5 years in *P. troglodytes*); stage II, at the end of the neurocranial growth phase (≈6 years in *H. sapiens* and 3 years in *P. troglodytes*); and stage III, adult (based on third molar eruption).

Factor Analysis. Factor analysis identifies combinations of variables that account for morphometric covariation among a given sample (19, 20). Although identified factors need to be further tested against *a priori* developmental models by using methods such as confirmatory factor analysis (21), exploratory factor analysis is a useful initial test of the hypothesis that a few structural modifications underlie much of the taxonomically important cranial variation in recent *Homo*. Factors were extracted from the AMHS as well as the combined AMHS and AH samples described above by using principal components analysis; both the initial factor solution and a varimax transformation were examined (20). Included variables quantify most of the previously proposed diagnostic characters of AMHS in Table 1: frontal angle, parietal angle, and occipital angle were measured following Howells (22); vault height relative to length was measured as basion-vertex/nasion-opisthocranion; vault width relative to height (measured as euryon–euryon/bregma–vertex) was substituted for bregma-asterion chord/biasterionic breadth (from ref. 1) because it better quantifies vault curvature in the coronal plane; canine fossa depth was measured as the maximum subtense between zygomaxillare and alare; supraorbital torus size/shape was quantified by using Lahr's system of grades (ref. 6, pp. 344–346); browridge length was calculated as the midsagittal distance from glabella to the bifrontomaxillare chord. Mandibular characters such as the chin and dental size measurements were not included in the analysis (see ref. 23).

Analysies of Variation. ANOVA and comparison of sample ranges were used to test the hypothesis that structural changes identified by the factor analysis discriminate between AH and AMHS. Because of unequal sample sizes, ANOVA significance was determined conservatively by using Scheffé's *F* (19). Variables compared include the previously proposed diagnostic cranial characters of AMHS (Table 1) and three additional variables included on the basis of the factor analysis results (see below) that have recently been proposed as structural determinants of AMHS cranial form (5–7, 14, 24–27): neurocranial globularity, defined as the roundedness of the cranial vault in the sagittal, coronal, and transverse planes; facial retraction, defined as the anteroposterior position of the face relative to the anterior cranial base and neurocranium; and facial prognathism, defined as the orientation of the lower face relative to the upper face. Table 2 provides details of how these variables were measured and standardized. Facial retraction could not be estimated reliably from external measurements, and was measured from radiographs and/or computed tomography scans of

Table 2. Comparison of facial projection, vault globularity, and other cranial features in archaic and anatomically modern *Homo*

	Recent *H. sapiens* ($n = 100$)			Pleistocene *H. sapiens* ($n = 9$)			Archaic *Homo* spp. ($n = 10$)			Overlap†,
Variable	Mean	SD	Range	Mean	SD	Range	Mean	SD	Range	%
Vault height relative to length (VHL)	0.76	0.04	0.68–0.90	0.74	0.04	0.67–0.80	0.63*	0.03	0.60–0.67	17
Parietal angle (PAA, degrees)	135.63	5.10	120–149	135.45	3.50	131–140	142.16*	7.41	133–155	83
Vault width relative to height (VWH)	0.98	0.07	0.81–1.15	0.95	0.06	0.89–1.07	0.85*	0.04	0.80–0.91	50
Occipital angle (OCA, degrees)	123.40	9.02	107–167	118.90	7.60	108–129	105.46*	8.23	96–117	40
Frontal angle (FRA, degrees)	129.49	6.26	102–145	128.44	3.59	121–131	139.54*	4.76	132–146	75
Browridge score (from ref. 6)	1.91	0.95	1–5	3.40	1.27	2–5	5.00*	0.00	5–5	100
Glabellar projection (mm)	24.02	4.29	11.4–34.8	24.47	4.39	17.3–29.8	32.79*	6.77	22.0–41.5	44
Canine fossa depth (mm)	4.82	1.74	1.8–10.1	4.75	1.17	3.5–6.3	1.74*	1.63	0–5.1	44
Prognathism (degrees)‡	35.89	4.35	27.7–52.8	35.84	2.69	32.6–40.2	34.37	3.21	30.1–41.4	100
Facial retraction/GM§	0.40	0.04	0.32–0.48	0.46	0.04	0.42–0.49	0.56*	0.03	0.51–0.58	0
Neurocranial globularity¶	0.59	0.06	0.49–0.86	0.58	0.04	0.51–0.61	0.47*	0.03	0.43–0.49	0

*Mean significantly different ($P < 0.05$, Scheffé's F, ANOVA) from combined AMHS sample (all variables distributed normally).
†Calculated as percentage of AH crania within total range of variation in combined AMHS sample.
‡The sagittal plane angle between prosthion, the most posteroinferior point on frontal squama above glabella, and the midline average of maxillary tuberosities.
§Measured as nasion–foramen cecum, standardized by a geometric mean of four cranial (mostly facial) dimensions: endocranial volume$^{0.33}$, nasion–prosthion, bimaxillary tuberosity breadth, and maxillary tuberosity–prosthion.
¶A dimensionless index of overall neurocranial globularity measured as (euryon-euryon·basion-vertex)/nasion-opsithocranion^2.

ANTHROPOLOGY

the comparative AMHS samples and those fossils for which nasion–foramen cecum can be measured: Bodo, Broken Hill, Cro Magnon I, Gibraltar I, Guattari, La Chapelle aux Saints, Obercassel I, Petralona, and Skhul V.

Geometric Morphometrics. To examine the structural and ontogenetic bases of differences in facial form between AH and AMHS, two morphometric analyses were calculated by using subsets of 17 landmarks digitized directly from computed tomography scans of fossil hominids measured ETDIPS (www.cc.nih.gov/cip/software/etdips/) and from radiographs of the ontogenetic samples of *H. sapiens* and *P. troglodytes*. Landmarks used were anterior nasal spine, basion, bregma, foramen cecum, glabella, lambda, nasion, opisthocranion, orbitale, pituitary point, posterior maxillary (PM) point, prosthion, sella, sphenoidale, the most inferoposterior midline point on frontal squama above glabella (frontex), and the midline points of greatest elevation between nasion and bregma (metopion), and bregma and lambda (see refs. 22 and 28 for landmark definitions). After Procrustes superimposition (29, 30), Thin Plate Spline (TPS) analysis (www.usm.maine.edu/%7Ewalker/; ref. 31) was used to visualize major differences in projected lateral view between taxa. Euclidean distance matrix analysis (EDMA) was also used to quantify significant differences in three-dimensional shape, by dividing all interlandmark lengths by a global geometric mean, and by using nonparametric bootstrapping ($n = 100$) to determine confidence intervals of 0.90 ($\alpha = 0.10$) for each size-corrected linear distance (32, 33).

Results

Exploratory Factor Analysis. Orthogonal and varimax solutions of both the AMHS and combined AMHS and AH samples yield virtually identical results, indicating similar, statistically robust patterns of covariation among the diagnostic features of AMHS listed in Table 1. Fig. 1 summarizes the initial (untransformed) factor solution of the AMHS sample in which factors 1–3 explain 61% of the sample variance. Variables that contribute substantially to factor 1 (factor scores > 0.50) are parietal angle, occipital angle, vault height relative to length, and vault height relative to width. These moderately correlated variables (mean $r = 0.40$ for the combined sample) all quantify cranial vault curvature in the coronal, sagittal, and transverse planes. As noted above, neurocranial globularity has previously been proposed to be diagnostic of AMHS (5, 6, 17, 24). In contrast, browridge size and frontal angle contribute to most of the variation in factor 2, and canine fossa depth explains most of the variation in factor 3. Of these patterns of covariation, the association between browridge size and frontal angle (factor 2) is related structurally to facial retraction, another key proposed structural autapomorphy of AMHS (24, 25). It has been well established that primates with more retracted faces have smaller, shorter browridges with steeper frontal squamae, reflecting the supraorbital region's role to integrate spatially the upper face and the neurocranium (see ref. 14); linear measurements of facial retraction explain ≈80% of browridge length and frontal angle variation across primates and in ontogenetic samples of humans and chimpanzees (25, 34). The structural basis for canine fossa depth, which contributes most of the variation in factor 3, is less clear and requires further study. Variation in this feature may be a function of maxillary arch retraction relative to the zygomatic, but could also reflect maxillary sinus expansion into the infraorbital region.

Analysis of Variation. Table 2 compares ranges and degrees of cranial variation for a number of features to test whether the two structural variables identified above, neurocranial globularity and facial retraction, discriminate between AH and AMHS better than the features traditionally thought to be diagnostic of AMHS. Although the mean values for all features in Table 1 differ significantly ($P < 0.05$) between the two samples, they do not completely separate AH and AMHS (see also refs. 7 and 8). Ranges overlap considerably for these variables, especially browridge size/shape and facial prognathism. However, measurements of facial retraction and vault globularity completely discriminate between the two taxa with no overlap (Table 2). Thus, as characters, neurocranial globularity and facial retraction appear to represent AMHS autapomorphies.

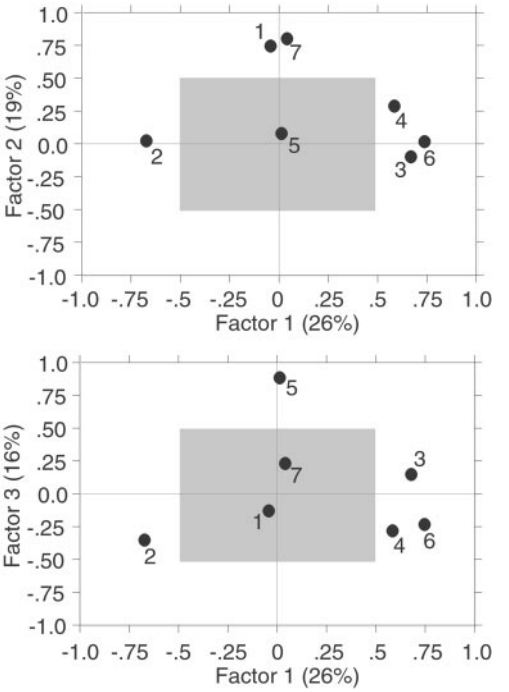

Fig. 1. Untransformed factor scores of external linear measurements (see *Materials and Methods*) that quantify most of the proposed diagnostic cranial characters of AMHS in Table 1. Variables are: 1, frontal angle (FRA); 2, parietal angle (PAA); 3, occipital angle (OCA); 4, vault width relative to height (VWH); 5, canine fossa depth (CFD); 6, vault height relative to length (VHL); and 7, browridge size/shape. Sample includes recent and fossil AMHS crania (see *Materials and Methods*). Variables outside the shaded box have factor loadings greater than 0.50. Factor 1 (which accounts for 26% of variance) separates variables that quantify neurocranial globularity; factors 2 and 3 (which together account for 35% of the variance) separate variables related to facial retraction. Factors from combined AMHS and AH samples (not shown here) show a similar pattern, but account for more sample variance.

Geometric Morphometric Comparisons. Variations in facial retraction are thought to be a function of interactions between several cranial components including facial size, cranial base angle, cranial base length, and brain size (14, 25–28). Likewise, variations in neurocranial globularity presumably derive from multiple interactions between portions of the brain and the size and shape of the cranial base (17, 28, 35). Thus, to better understand the origin of AMHS cranial form it is useful to identify more proximate variables that interact during growth to generate variations in facial retraction and neurocranial globularity among recent humans. As a preliminary effort, we first used TPS and EDMA analyses of landmarks that include major loci of cranial growth to compare the pattern of shape differences between adult AMHS and two taxa of AH: Neanderthals and African archaic *Homo*. The results, summarized in Fig. 2, not only highlight the above described differences in facial retraction and neurocranial globularity, but also reveal several important differences in facial and cranial base shape that provide clues about their structural and developmental causes. The most obvious difference is that the AMHS face is much smaller relative to overall cranial size than in either group of AH. According

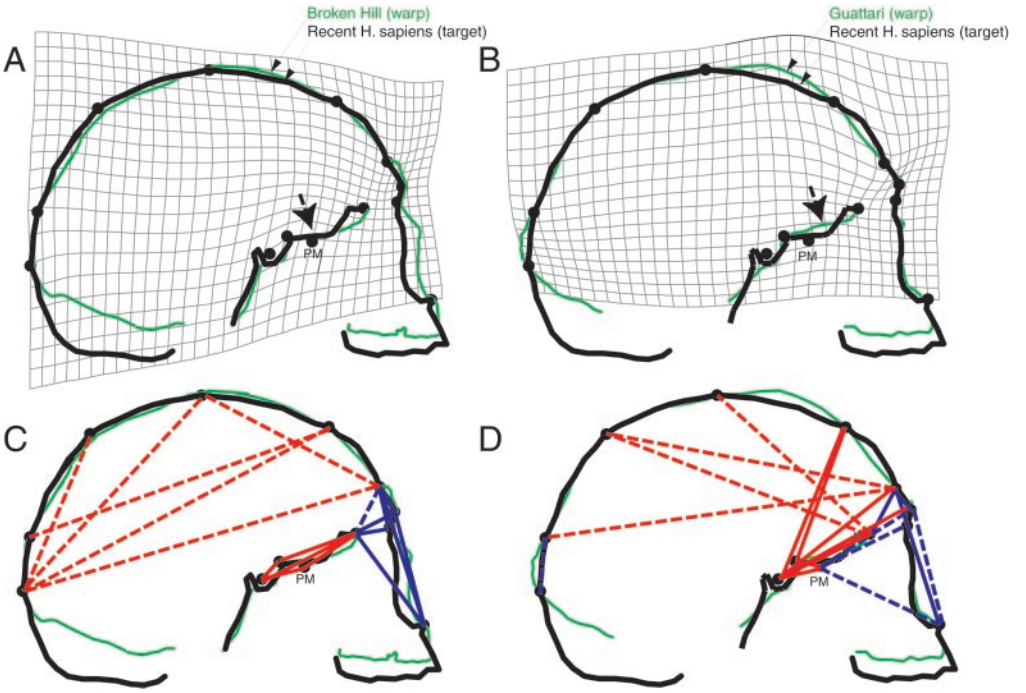

Fig. 2. Geometric morphometric comparisons of AH and AMHS cranial form. (*A* and *B*) TPS analysis based on least-squared superimposition (see *Materials and Methods*) of modern human (target) and Broken Hill (warp, in green; *A*), and Guattari (warp, in green; *B*). Landmarks used in TPS: sella, sphenoidale, PM point, foramen cecum, anterior nasal spine, nasion, glabella, bregma, lambda, opisthocranion, the most inferoposterior midline point on frontal squama above glabella (frontex), the midline point of greatest elevation between nasion and bregma (metopion), and the midline point of greatest elevation between bregma and lambda (see *Materials and Methods* for definitions). Arrows indicate basicranial flexion in warp. (*C* and *D*) EDMA of four modern humans versus Broken Hill and Bodo (*C*) and Guattari and Gibraltar 1 (*D*). Red lines indicate scaled linear distances ≥10% longer in AMHS than warp crania; blue lines indicate scaled linear distances ≥10% shorter in AMHS than warp crania; dashed lines indicate linear distances calculated by using only Broken Hill (*C*) or Guattari (*D*) from a smaller subset of landmarks. Note that the PM point, the most anterior point on the greater wings of the sphenoid, lies off the midsagittal plane.

to the landmarks used here, facial reduction in AMHS appears to be concentrated in the upper face, with 10–15% decreases in both supero-inferior height and antero-posterior length relative to overall cranial size. AMHS also have smaller midfaces than Neanderthals but not the archaic Africans because of autapomorphic midfacial prognathism in Neanderthals (2).

At least three important differences in shape between the AMHS and AH samples are also evident in the cranial base. First, anterior cranial base length (e.g., from sella to foramen cecum) is ≈15–20% longer relative to overall cranial size in AMHS than in either taxon of AH. Second, the anterior cranial base (and with it the face) is more flexed relative to the posterior cranial base in AMHS (as indicated by arrows in Fig. 2; see also refs. 25 and 28). Average cranial base angle in AMHS is 134° (ref. 18), but is ≈15° more extended in Guattari and Broken Hill. Third, the EDMA analyses indicate that the middle cranial fossa in AMHS is ≈20% wider relative to overall cranial size, as shown by the distance between the midline of the sphenoid body and the poles of the temporal lobes (the PM points). These differences in relative cranial fossae dimensions suggest that the temporal (and possibly the frontal) lobes are proportionately larger in AMHS than AH.

Although the above analyses suggest that a few variables may underlie major cranial shape differences between AH and AMHS, further analyses are necessary to test whether and how growth differences explain these contrasting patterns, especially in terms of facial retraction and neurocranial globularity. Recent geometric morphometric comparisons (36) show that Neanderthal and AMHS crania have distinctive, ontogenetically early growth patterns that may result from shifts in basicranial and facial development. However, the available sample of infant AH crania is too small and insufficiently complete, particularly in the basicranium, to test directly the effects of facial size, cranial base flexion, anterior cranial base length, and middle and anterior cranial fossae size on cranial ontogeny. In addition, there are no well-preserved fossil Neanderthal crania with undistorted or complete cranial bases, and none younger than 2.2 postnatal years, by which time most cranial base growth (e.g., flexion) is complete (18).

An alternative, preliminary way to test the effects of facial diminution, cranial base flexion, anterior cranial base elongation, and expansion of the middle and anterior cranial fossae on facial retraction and neurocranial globularity in *H. sapiens* is to compare ontogenetic samples of human and nonhuman primates to test whether the same variables contribute to homologous structural differences. This hypothesis is supported by the analyses summarized in Fig. 3, which compare cranial ontogeny in humans and chimpanzees by using just the cranial base and facial landmarks from the analysis presented in Fig. 2. Fig. 3 shows that, in contrast to humans, facial retraction decreases during *Pan* ontogeny. During early postnatal ontogeny (between stages I and II), facial projection is associated with a decrease in the relative length of the anterior and middle cranial fossae and with an increase in relative facial length and height (Fig. 3*A*). After neural growth is complete in *Pan* (between stages II and III), the relative lengths of the cranial fossae continue to shorten, facial height and length continue to increase, and the cranial base extends, rotating the face dorsally relative to the neurocranium (Fig. 3*B*; refs. 18 and 28). In contrast, development of relative cranial base length, relative facial size, and cranial base angulation is different in *H. sapiens* ontogeny, as the neurocranium remains highly globular and the face stays retracted under the anterior cranial base. Between stages I and II (while the brain is still growing but cranial base flexion is complete; ref. 18), the posterior cranial fossa becomes relatively shorter as facial size remains constant relative to overall cranial size (Fig. 3*C*). As the human face increases in relative size (mostly inferiorly) between

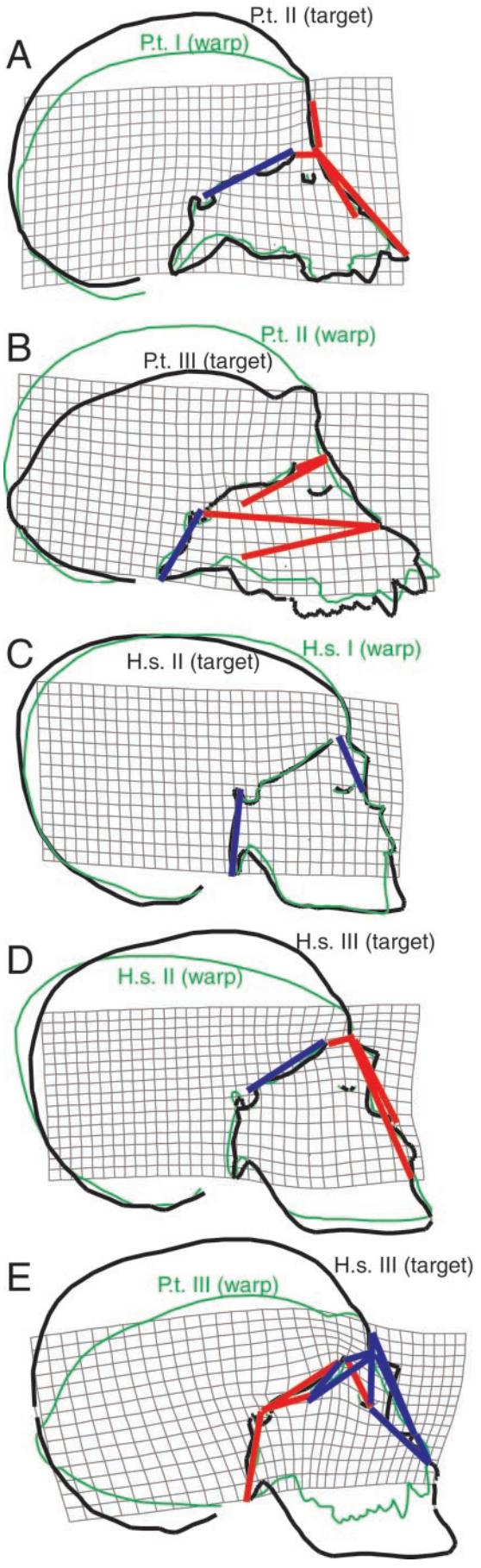

stages II and III, facial retraction decreases slightly, the anterior cranial fossa becomes relatively shorter, and the cranial base remains flexed rather than extending as it does in *Pan* (Fig. 3*D*). Basicranial flexion is important because it positions most of the face beneath the anterior cranial fossa. In conclusion, the major variables that apparently underlie differences in facial retraction and neurocranial globularity between AH and AMHS are the same ones that contribute to similar differences evident in human and chimpanzee cranial ontogeny: cranial base angle, the relative length and width of the cranial fossae, and relative facial height and length (Fig. 3*E*).

Discussion

The above results indicate that most of the differences previously identified between AH and AMHS crania relate to changes in facial retraction and overall neurocranial globularity. These two structural modules not only explain much of the covariation among traditional diagnostic features of AMHS (1–4), but also do a better job of discriminating AH and AMHS crania (see refs. 6–8). Additional crania are needed to test this hypothesis more extensively, but in the diverse sample studied here, there was no overlap in the range of variation of quantitative measures of these features. Facial retraction and neurocranial globularity probably discriminate between AH and AMHS human crania better than Day and Stringer's (1) characters because of the effects of integration. Most of the characters in Table 1 are not independent, but instead measure aspects of neurocranial shape, facial retraction and other features that reflect morphological integration during growth among basic structural units of the skull (e.g., nasal and oral pharynges, eyeballs, neural lobes, etc.). As a working hypothesis that requires further testing, we propose that only fossil crania with an index of neurocranial globularity greater than 0.50 and an index of facial retraction less than 0.50 should be classified as *H. sapiens*. We caution, however, that such criteria are not applicable to artificially deformed or otherwise pathological crania such as WLH 50 (37).

Although facial retraction and neurocranial globularity appear to be AMHS autapomorphies, they are not independent units—what Wagner (38) terms biological characters—but are instead structural modules that likely derive from complex interactions among more fundamental units of the skull. Determining the proximate causes of these autapomorphies is speculative without a more sophisticated understanding of cranial morphogenesis and without enough well-preserved infant and juvenile crania to compare directly cranial ontogeny in AH and AMHS. However, it is reasonable to hypothesize that the evolution of AMHS cranial form may have been caused by changes in just a few variables that influence the relative spatial position of the face, cranial base, and neurocranium. The most important of these shifts are increased flexion of the cranial base, a longer anterior cranial base, a shorter face (especially anteroposterior length), and, possibly, increased size of the temporal and/or frontal lobes relative to other parts of the skull. Ontogenetic and interspecific studies demonstrate the effects of these variables on cranial shape among human and nonhuman

Fig. 3. Ontogenetic TPS and EDMA analyses of cranial growth in *Pan* and *Homo* (see *Materials and Methods* for details). Outlines are selected specimens (targets in black, warps in green). (*A*) *P. troglodytes* stage II (target), stage I (warp). (*B*) *P. troglodytes* stage III (target), stage II (warp). (*C*) *H. sapiens* stage II (target), stage I (warp). (*D*) *H. sapiens* stage III (target), stage II (warp). (*E*) Stage III *H. sapiens* (target), stage III *P. troglodytes* (warp). The TPS analysis is based on only basicranial and facial landmarks: basion, prosthion, anterior nasal spine, nasion, glabella, opisthocranion, sella, pituitary point, sphenoidale, posterior maxillary plane point, foramen cecum, orbitale, and posterior nasal spine. Superimposed on TPS are EDMA results: red lines indicate scaled linear distances that are significantly longer in target than warp crania; blue lines indicate scaled linear distances that are significantly shorter in target than warp crania.

primates. Increased cranial base flexion relative to cranial base length and brain size is associated with increased globularity of the brain, hence of the braincase (24, 35, 39, 40). Moreover, because the cranial base floor is the roof of the face, cranial base flexion influences facial orientation relative to the anterior cranial fossa (reviewed in ref. 28), and anteroposterior facial length relative to anterior cranial base length affects facial projection relative to the neurocranium (reviewed in ref. 14). In addition, temporal and frontal lobe sizes influence the size of the middle and anterior cranial fossae, respectively. Expansion of either lobe thus lengthens the anterior cranial base (see above). Finally, increases in relative temporal lobe size also contribute to reorienting the face more vertically underneath the anterior cranial fossa because the most anterior points of the middle cranial fossae (the PM points) lie on the posterior margin of the face, the PM plane, which has been shown to be tightly constrained (90°) relative to the orientation of the axis of the orbits within humans and between primates (28, 41). Thus, temporal lobe elongation relative to cranial size rotates the entire face below the anterior cranial fossa (reviewed in ref. 28).

Futher comparative and ontogenetic analyses are needed to test more fully the effects of cranial base flexion, anterior cranial base length, facial length, and temporal and/or frontal lobe size on facial retraction and neurocranial globularity in *Homo*. In addition, it would be interesting to know more about the proximate causes of these changes, and their possible adaptive bases (if any). As noted above, increases in relative temporal and frontal lobe size probably cause relative elongation of the anterior cranial base in AMHS, and may also underlie increased basicranial flexion (28). It is intriguing but still premature to speculate whether such neural differences relate to possible behavioral differences between AH and AMHS (42).

Regardless of their cause, the existence of several AMHS autapomorphies has clear systematic implications. Although a universally acceptable definition of the species unit is a quixotic endeavor, both phylogenetic and evolutionary species concepts agree that species should be monophyletic lineages, evolving separately from other lineages (43, 44). If one accepts a lineage-based species concept, then AMHS autapomorphies are persuasive evidence that *H. sapiens* is a distinct species from AH taxa, including the Neanderthals (*H. neanderthalensis*) and fossils sometimes attributed to *H. heidelbergensis*, *H. rhodesiensis*, or other hypodigms. Another likely noncranial autapomorphy of *H. sapiens* (not analyzed here) may be the chin (see ref. 23).

In addition, from a developmental perspective, many of the variables that influence facial retraction and neurocranial globularity (cranial base angle and temporal and frontal lobe size) may be good systematic characters because they develop early in ontogeny, and because they likely have a low degree of phenotypic plasticity. In fact, several recent studies show that the major differences in cranial growth between Neanderthals and AMHS arise prenatally or perinatally (36). One interesting exception, however, may be facial size, which grows more slowly during ontogeny and which is partially subject to epigenetic effects from mastication (45). Variations in facial size probably contribute to much of the variation in browridge size and other correlates of facial retraction evident within recent *H. sapiens* (5, 6, 14, 17).

We have much to learn about the complex processes of cranial growth and integration, but the above results highlight how efforts to tease apart these processes have the potential to yield better characters for testing systematic hypotheses, and to identify possible targets of selection during speciation. It is exciting to consider that only a few small shifts in growth, probably in the brain and possibly in the cranial base, may be responsible for most aspects of the evolution of modern human cranial form. Viewed in this light, the origin of modern human cranial form is more likely a result of relatively minor morphogenetic "tinkering" than a major shift in developmental processes.

We thank C. Dean, J. Jernvall, P. O'Higgins, G. Manzi, D. Pilbeam, R. Potts, F. Spoor, and several anonymous reviewers for helpful comments; K. Mowbray, G. Sawyer, I. Tattersall, and M. Morgan for access to skeletal collections; and D. Hunt, B. Frohlich, J.-J. Hublin, R. Machiarelli, M. Ponce de León, H. Seidler, F. Spoor, C. Stringer, and C. Zollikofer for access to CT scans and/or radiographs of fossils.

1. Day, M. H. & Stringer, C. B. (1982) in *L'*Homo erectus *et la place de l'homme de Tautavel parmi les hominides fossiles*, ed. De Lumley, M.A. (Centre National de la Recherche Scientifique, Nice, France), pp. 814–846.
2. Stringer, C. B., Hublin, J. J. & Vandermeersch, B. (1984) in *The Origins of Modern Humans: A World Survey of the Fossil Evidence*, eds. Smith, F. H. & Spencer, F. (Liss, New York), pp. 51–135.
3. Groves, C. P. (1989) *A Theory of Human and Primate Evolution* (Oxford Univ. Press, Oxford).
4. Tattersall, I. (1992) *J. Hum. Evol.* **22,** 341–349.
5. Lieberman, D. E. (1995) *Curr. Anthropol.* **36,** 159–197.
6. Lahr, M. M. (1996) *The Evolution of Modern Human Diversity: A Study of Cranial Variation* (Cambridge Univ. Press, Cambridge).
7. Wolpoff, M. (1986) *Anthropos (Brno)* **23,** 41–53.
8. Kidder, J. H., Jantz, R. L. & Smith, F. H. (1992) in *Continuity or Replacement: Controversies in Homo sapiens Evolution*, eds. Bräuer, G. & Smith, F. H. (Balkema, Rotterdam), pp. 157–177.
9. Wolpoff, M. H., Hawks, J., Frayer, D. W. & Hunley, K. (2001) *Science* **291,** 293–297.
10. Krings, M., Capelli, C., Tschentscher, F., Geisert, H., Meyer, S., von Haeseler, A., Grossschmidt, K., Possnert, G., Paunovic, M. & Pääbo, S. (2000) *Nat. Genet.* **26,** 144–146.
11. Ovchinnikov, I. V., Gotherstrom, A., Romanova, G. P., Kharitonov, V. M., Liden, K. & Goodwin, W. (2000) *Nature (London)* **404,** 490–493.
12. Adcock, G. J., Dennis, E. S., Easteal S., Huttley, G. A., Jermiin, L. S., Peacock, W. J. & Thorne, A. (2001) *Proc. Natl. Acad. Sci. USA* **98,** 537–542.
13. Atchley, W. R. & Hall, B. K. (1991) *Biol. Rev. Camb. Philos. Soc.* **66,** 101–157.
14. Lieberman, D. E. (2000) in *Development, Growth and Evolution*, eds. O'Higgins, P. & Cohn, M. (Academic, London), pp. 85–122.
15. Raff, R. (1996) *The Shape of Life* (Univ. Chicago Press, Chicago).
16. Carroll, S. B., Grenier, J. K. & Weatherbee, S. D. (2001) *From DNA to Diversity* (Blackwell, Oxford).
17. Lieberman, D. E., Pearson, O. M. & Mowbray, K. M. (2000) *J. Hum. Evol.* **38,** 291–315.
18. Lieberman, D. E. & McCarthy, R. C. (1999) *J. Hum. Evol.* **36,** 487–517.
19. Sokal R. R. & Rohlf, F. J. (1995) *Biometry* (Freeman, San Francisco), 2nd Ed.
20. Reyment, R. A. & Jöreskog, K. H. (1993) *Applied Factor Analysis in the Natural Sciences* (Cambridge Univ. Press, Cambridge, U.K.), 2nd Ed.
21. Zelditch, M. L. (1987) *Syst. Zool.* **36,** 368–380.
22. Howells, W. W. (1973) *Cranial Variation in Man: A Study by Multivariate Analysis of Patterns of Difference Among Recent Populations* (Peabody Museum Bulletin, Cambridge, MA).
23. Schwartz, J. H. & Tattersall, I. (2000) *J. Hum. Evol.* **38,** 367–409.
24. Weidenreich, F. (1941) *Trans. Am. Philos. Soc.* **31,** 321–442.
25. Lieberman, D. E. (1998) *Nature (London)* **393,** 158–162.
26. Spoor, F., O'Higgins, P., Dean, M. C. & Lieberman, D. E. (1999) *Nature (London)* **397,** 572 (lett.).
27. O'Higgins, P. (1999) in *On Growth and Form: Spatio-temporal Pattern Formation in Biology*, eds. Chaplain, M., Singh, G. D. & McLachlan, J. C. (Wiley, New York), pp. 373–393.
28. Lieberman, D. E., Ross, C. F. & Ravosa, M. J. (2000) *Yearbook Phys. Anthropol.* **43,** 117–169.
29. Chapman, R. E. (1990) in *Proceedings of the Michigan Morphometrics Workshop*, eds. Rohlf, F. J. & Bookstein, F. L. (Univ. Michigan Museum of Zoology, Ann Arbor), pp. 251–267.
30. Rohlf, F. J. (1990) in *Proceedings of the Michigan Morphometrics Workshop*, eds. Rohlf, F. J. & Bookstein, F. L. (Univ. Michigan Museum of Zoology, Ann Arbor), pp. 227–236.
31. Bookstein, F. L. (1989) *IEEE Trans. Pat. Anal. Mac. Intel.* **11,** 567–585.
32. Lele, S. (1993) *Math. Geol.* **25,** 573–602.
33. Lele, S. & Richstmeier, J. T. (1995) *Am. J. Phys. Anthropol.* **98,** 73–86.
34. Ravosa, M. J. (1991) *Am. J. Phys. Anthropol.* **86,** 369–396.
35. Enlow, D. H. (1990) *Facial Growth* (Saunders, Philadelphia), 3rd Ed.
36. Ponce de León, M. S. & Zollikofer, C. P. E. (2001) *Nature (London)* **412,** 534–538.
37. Webb, S. G. (1990) *Am. J. Phys. Anthropol.* **82,** 403–411.
38. Wagner, G. P. (2001) in *The Character Concept in Evolutionary Biology*, ed. Wagner, G. P. (Academic, San Diego), pp. 1–10.
39. Ross, C. & Henneberg, M. (1995) *Am. J. Phys. Anthropol.* **98,** 575–593.
40. Hofer, H. (1969) *Ann. N.Y. Acad. Sci.* **162,** 341–356.
41. McCarthy, R. C. & Lieberman, D. E. (2001) *Anat. Record* **264,** 247–260.
42. McBrearty, S. & Brooks, A. S. (2000) *J. Hum. Evol.* **39,** 453–563.
43. Simpson, G. G. (1961) *Principles of Animal Taxonomy* (Columbia Univ. Press, New York).
44. Cracraft, J. (1983) *Curr. Ornithol.* **1,** 159–187.
45. Herring, S. W. (1993) in *The Skull*, eds. Hanken, J. & Hall, B. K. (Univ. Chicago Press, Chicago), Vol. 1, pp. 153–206.